NJC

Accepted Manuscript

This article can be cited before page numbers have been issued, to do this please use: R. Misra, R. Sharma and R. Maragani, *New J. Chem.*, 2017, DOI: 10.1039/C7NJ03934D.

This is an Accepted Manuscript, which has been through the Royal Society of Chemistry peer review process and has been accepted for publication.

Accepted Manuscripts are published online shortly after acceptance, before technical editing, formatting and proof reading. Using this free service, authors can make their results available to the community, in citable form, before we publish the edited article. We will replace this Accepted Manuscript with the edited and formatted Advance Article as soon as it is available.

You can find more information about Accepted Manuscripts in the author guidelines.

Please note that technical editing may introduce minor changes to the text and/or graphics, which may alter content. The journal's standard Terms & Conditions and the ethical guidelines, outlined in our author and reviewer resource centre, still apply. In no event shall the Royal Society of Chemistry be held responsible for any errors or omissions in this Accepted Manuscript or any consequences arising from the use of any information it contains.

ROYAL SOCIETY OF CHEMISTRY

rsc.li/njc

View Article Online
DOI: 10.1039/C7NJ03934D

C_3-Symmetric Star Shaped Donor-Acceptor Truxenes: Synthesis, Photophysical, Electrochemical and Computational Studies

Rekha sharma, Ramesh Maragani, Rajneesh Misra*

Abstract:

This manuscript reports the design and synthesis of C_3-symmetric star shaped donor and acceptor substituted truxenes **6**, **7, 10** and **11** using Pd-catalyzed Sonogashira cross-coupling and [2+2] Cycloaddition-retroelectrocyclization reactions. Their photophysical, electrochemical and computational studies were explored, which exhibits strong donor-acceptor interaction and effective tuning of the HOMO–LUMO gap. The computational studies reveal that the TCNE and TCNQ substituted truxenes **10** and **11** exhibit lower HOMO–LUMO gap compared to truxene **6** and **7**. The reaction pathway of [2+2] cycloaddition-retroelectrocyclization was studied by computational calculations, which reveals that, the donor substituted truxene **7** is favourable whereas acceptor substituted truxene **6** is not favourable for cycloaddition-retroelectrocyclization reactions.

Introduction:

The development of novel π□conjugated donor–acceptor (D–A) molecular systems have drawn immense attention of the scientific community due to their potential applications in multi-photon absorption, organic light emitting diodes (OLEDs) and organic field effect transistors (OFETs), organic photovoltaics (OPVs).[1,2] The electronic and photonic properties of the π□conjugated D–A molecular systems can be tuned by altering the HOMO□LUMO gap.[3] The HOMO□LUMO gap in D–π–A molecular systems can be tuned either by altering the strength of D/A units or by varying the π-bridge.[4,5]

The D–A systems incorporating the cyano-based acceptors such as tetracyanoethylene (TCNE) and 7,7,8,8-tetracyanoquinodimethane (TCNQ) are potential candidates for dye-

View Article Online
DOI: 10.1039/C7NJ03934D

sensitized solar cells (DSSCs), organic photovoltaics and non-linear optics.[6–8] Diederich and others have reported the synthesis and properties of various TCNE and TCNQ substituted derivatives using [2+2] cycloaddition–retroelectrocyclization reaction.[9a–c] Michinobu *et al*. have explored the TCNE and TCNQ substituted polymers which are promising materials for photovoltaic applications.[9d,e] Shoji *et al*. have reported donor–acceptor based TCNE and TCNQ molecules as a redox active ICT chromophores. [9f,g] Butenschoen *et al.* have synthesized a variety of 1,1´-disubstituted ferrocenyl TCBD derivatives.[9h] Our group is interested in the design and synthesis of novel D–A molecular systems for optoelectronic applications.[10]

The star-shaped truxene is a rigid building block for constructing extended π-conjugated molecular systems due to its easy functionalization, excellent solubility, high thermal and chemical stability.[11–13] Jian Pei *et al.* have explored various star shaped π-conjugated molecules based on the truxene core for optoelectronic applications.[12,14] Literature reveals that truxene based donor–acceptor systems have potential applications in organic light-emitting diodes (OLED), organic solar cells (OSC) and organic fluorescent probes.[15–17]

Recently, we have explored the reaction pathway and tuning of HOMO-LUMO gap of TCNE functionalized bisthiazole based donor-acceptor systems.[21] We were further interested to study the [2+2] cycloaddition-retroelectrocyclization reaction pathway and tuning of HOMO-LUMO energy gap of triphenylamine (donor), naphthalimide (acceptor) substituted truxene and their TCNE and TCNQ derivatives. The triphenylamine and naphthalimide substituted truxenes were synthesized by the Pd-catalyzed Sonogashira cross-coupling reaction and their photophysical, electrochemical and computational studies were performed. The triphenylamine (donor) substituted truxene **7** was further subjected to the [2+2] cycloaddition–retroelectrocyclization reaction with tetracyanoethylene (TCNE) and 7,7,8,8-

View Article Online
DOI: 10.1039/C7NJ03934D

tetracyanoquinodimethane (TCNQ), which resulted in truxenes **10** and **11**. On the other hand the naphthalimide (acceptor) substituted truxene **6** does not undergo the cycloaddition retroelectrocyclization reaction due to the lower HOMO and higher LUMO energy level of TCNE.[18]

Results and discussion:

The donor (TPA) and acceptor (NDI) substituted substituted truxenes **6**, **7, 10** and **11** were synthesized by the Pd-catalyzed Sonogashira cross-coupling reaction and [2+2] cycloaddition-retroelectrocyclization reactions (Scheme **2**). The truxene **1** was synthesized by 1-indanone in the presence of acetic acid and hydrochloric acid.[19] Truxene exhibits poor solubility due to its flat disc like conformation. Therefore, in order to improve the solubility six hexyl groups were attached to the C-5, C-10, and C-15 positions of the truxene moiety by alkylation reaction using bromo-hexane, which resulted readily soluble hexahexylated truxene **2** (Scheme **1**).[19] The iodination reaction of truxene **2** in the presence of HIO_3 and I_2 resulted in tri-iodo truxene **3** in 80% yield (Scheme **1**).[20]

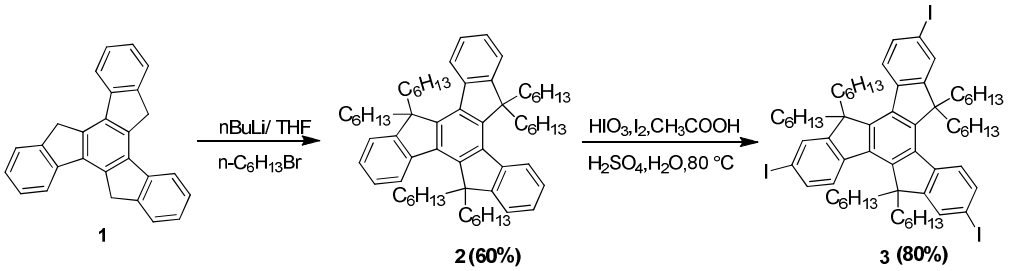

Scheme **1**: Synthesis of tri-iodotruxene **3**.

View Article Online
DOI: 10.1039/C7NJ03934D

The intermediates 4-ethynyl-N,N-diphenylaniline (**5**), 4-ethynyl-1,8-naphthalimide (**4**) were synthesized by reported procedure.[21] To overcome the solubility problem n-butyl group was attached at the N-position of 4-ethynyl-1,8-naphthalimide. The reaction of tri-iodo truxene **3** with 4-ethynyl-1,8-naphthalimide **4**, 4-ethynyl-N,N-diphenylaniline **5** under the catalytic system $Pd(dba)_2/AsPh_3$ resulted truxene **6** and **7** in 70% and 75% yield respectively (Scheme **2**). The triphenylamine substituted truxene **7** was further subjected to the [2+2] cycloaddition-retroelectrocyclization reactions with TCNE and TCNQ at 100 ^{o}C for 16 h, which resulted truxene **10** and **11** in 71%, and 65% yield respectively. The reaction of naphthalimide substituted truxene **6** with TCNE and TCNQ did not lead to the product formation (Scheme **2**). The truxenes **6**, **7, 10** and **11** showed good solubility in common organic solvents and were well characterized by ^{1}H NMR, ^{13}C NMR, and HRMS techniques.

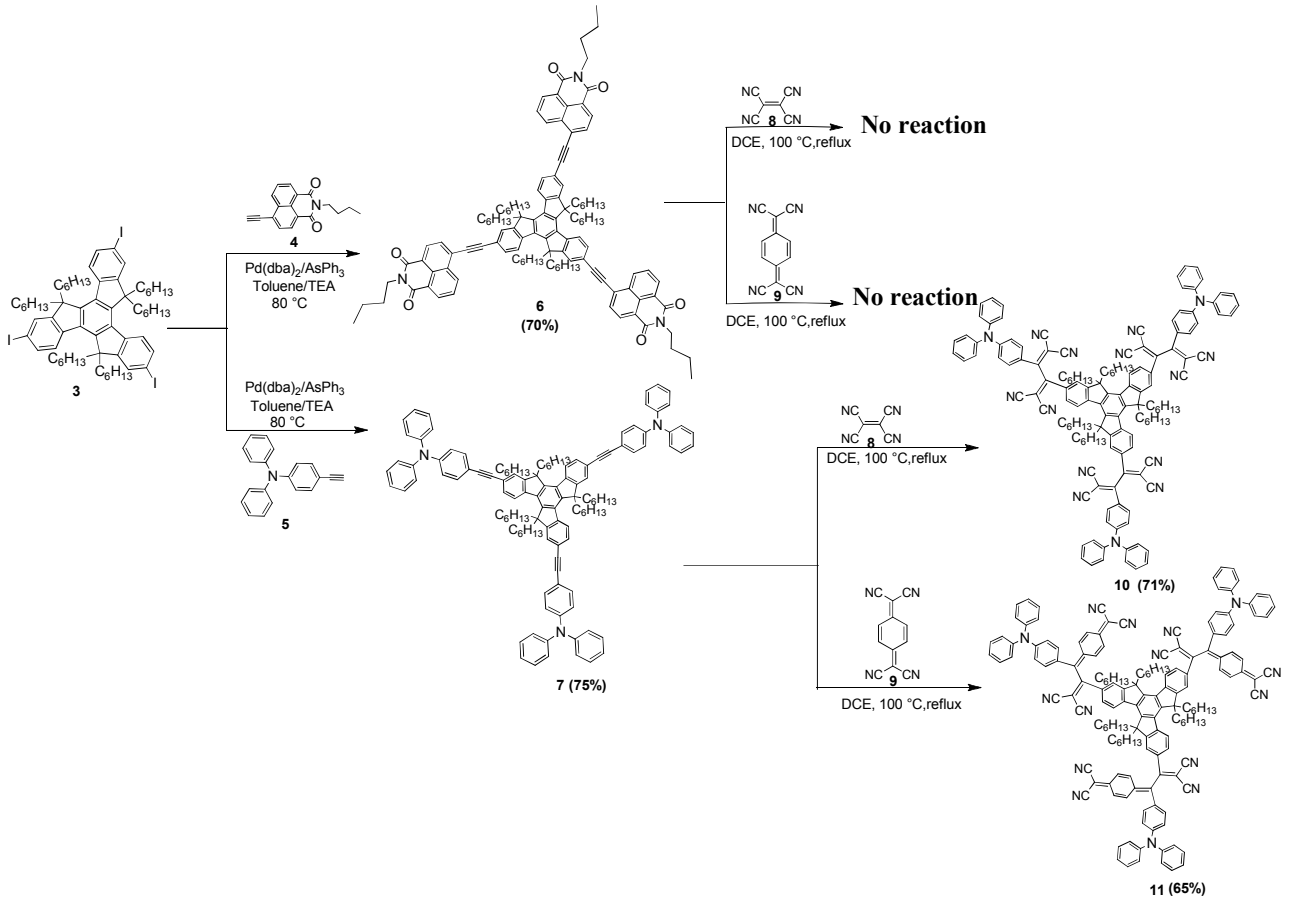

Scheme **2**: Synthesis of donor/acceptor substituted truxenes **6**, **7, 10** and **11.**

View Article Online
DOI: 10.1039/C7NJ03934D

The triphenylamine substituted truxene **7** undergoes cycloaddition reaction with TCNE as shown by negative Gibbs free energy -0.14 kcal/mol calculated by computational studies, shown in Figure **1**. In case of naphthalimide substituted truxene **6** the cycloaddition reaction was unsuccessful as shown by positive Gibbs free energy (0.59 kcal/mol).[22] This confirms that donor substituted truxenes are favourable for cycloaddition reaction, whereas truxenes substituted by electron withdrawing groups are not favourable (Figure **1**).

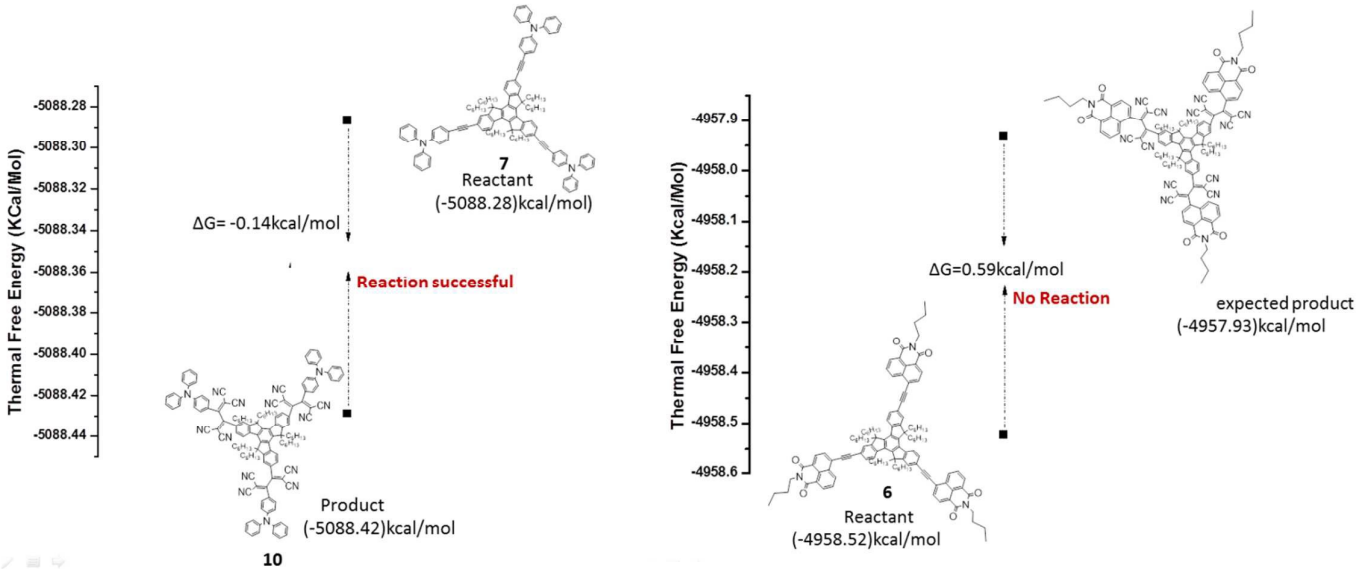

Figure 1. The Gibbs free energy differences of the truxenes **6** and **7** by using 6-311+ g(d,p)/ B3LYP at 100 °C in 1,2-dichloroethane solvent.

In triphenylamine substituted truxene (**7**) the HOMO energy level (-4.99 eV) is closer to the LUMO level of TCNE (-4.56 eV) as compared to HOMO energy level of truxene **6** (-5.68 eV) (Figure **2**). Therefore overlapping of HOMO orbital of truxene **7** and LUMO orbital of TCNE is feasible in cycloaddition reaction whereas the overlapping of orbitals between TCNE and truxene **6** is not favourable.[23]

View Article Online
DOI: 10.1039/C7NJ03934D

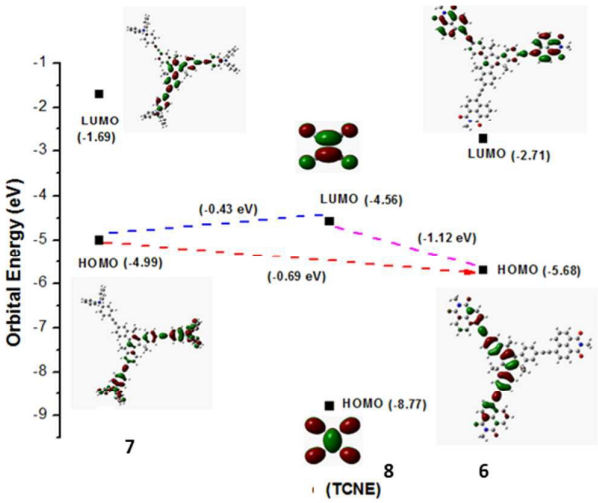

Figure 2. The HOMO and LUMO molecular orbitals of truxene **7**, TCNE and truxene **6** by using 6-311^{+} g(d,p)/B3LYP at 100 °C in 1,2-dichloroethane solvent.

The thermal stability of the donor and acceptor substituted truxenes **6**, **7, 10** and **11** were explored using thermogravimetric analysis (TGA) at a heating rate of 10 °C min^{-1} under nitrogen atmosphere (Figure **3**). The decomposition temperature for 10% weight loss in truxenes **6–11** were above 370 °C. The naphthalimide substituted truxene **6** showed better thermal stability, as the 10% weight loss is at higher temperature (426 °C) as compared to other truxenes (Table **1**). The overall thermal stability of truxenes follow the order **6** > **7** > **11** > **10.**

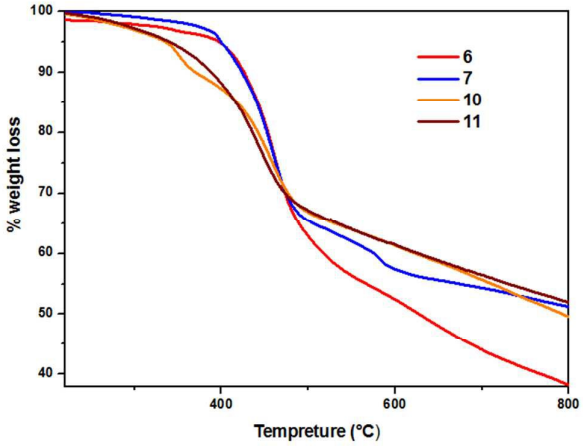

Figure 3. TGA plots of truxenes **6**, **7, 10** and **11**

View Article Online
DOI: 10.1039/C7NJ03934D

Photophysical properties:

The UV-vis absorption spectra of the truxenes **6**, **7, 10** and **11** were recorded in dichloromethane at room temperature (Figure **4**), and the data are listed in Table **1**. The truxenes exhibit absorption band between 273–320 nm corresponding to π-π* transition. The absorption spectra of truxene **6** and **7** exhibit charge transfer (CT) band at 418 nm and 383 nm respectively. In truxene **10**, the incorporation of TCNE unit results in red shifted strong charge transfer band at 433 nm whereas TCNQ acceptor unit result in multi-CT bands in truxene **11**.[24] This indicates strong donor–acceptor interaction in truxene **10** and **11** with TCNE and TCNQ linkers. The presence of strong CT transition results in intense colour solution of truxenes **6–11** in dichloromethane (Figure **5**).

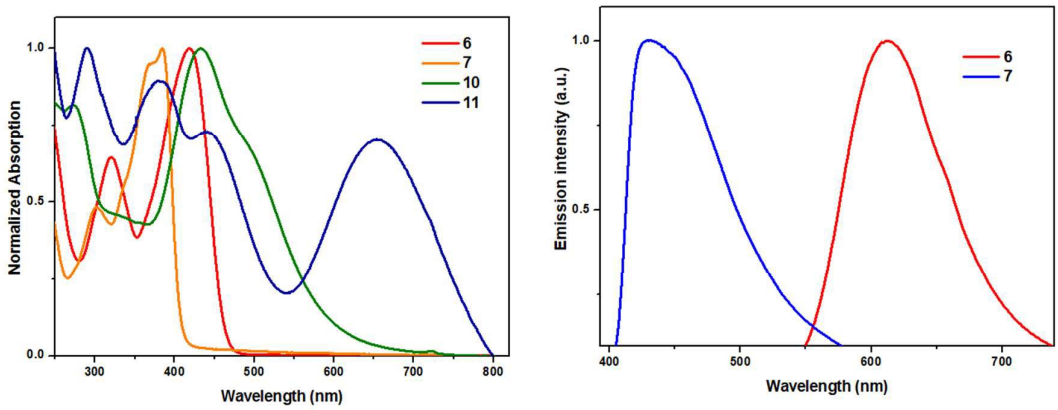

Figure 4: (a) Normalized electronic absorption spectra of truxene **6**, **7, 10** and **11** and (b) fluorescence spectra of truxenes **6** and **7** (1.0×10^{-5} M concentration) in dichloromethane.

The trend observed in the HOMO–LUMO gap values exhibit the order **7**>**6**>**10**>**11**. This reveals that the HOMO–LUMO gap values were considerably lowered in the TCNQ linked truxene **11** followed by the TCNE substituted truxene **10** and naphthalimide substituted truxene **6**. Hence, HOMO□LUMO gap in these truxene derivatives are function of the acceptor strength. The fluorescence emission wavelengths for truxenes **6** and **7** were observed

View Article Online
DOI: 10.1039/C7NJ03934D

at 611 nm and 430 nm respectively (Table **1**). The TCNE and TCNQ linked truxenes **10** and **11** are non-emissive in nature.[25,26]

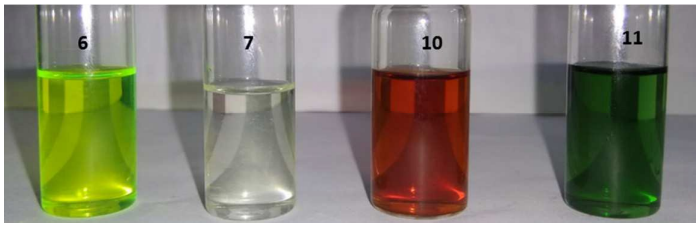

Figure 5: Truxenes **6**, **7, 10** and **11** at 1×10^{-5} M concentration in dichloromethane in day light.

Table 1. Photophysical and electrochemical data of truxenes **6**, **7, 10** and **11**

Compound	Photophysical data[a] λ_{max}, [nm] ($\varepsilon \times 10^5$[mol^{-1}cm^{-1}])	Emission λ_{max}[nm][a]	Φ_f[b]	Electro-chemical data[c] E_{ox}(V)	E_{red}(V)	Theoretical HOMO-LUMO gap (eV)	[d]T_d °C
Ferrocene	-	-	-	0.00	-		
6	320(1.1), 418	611	0.42	1.31	-1.47	2.98	426
7	300(1.2), 383	430	0.54	0.37 0.96	-1.44	3.31	424
10	273(1.5), 433	-	-	1.30	-1.49	2.34	370
11	290(1.8), 380, 440, 655	-	-	1.25	-1.46	1.92	388

[a]Measured in DCM at T = 25 °C, λ_{max} (nm): absorption maximum. ε, extinction coefficient. [b] Determined by using quinine sulphate as a standard (Φ^{st} = 0.54). [c]Recorded by cyclic voltammetry using 1.0×10^{-3} M solutions of **6–11** containing 0.1 M solution of Bu_4NPF_6 in DCM at 100 mV s^{-1}scan rate, vs. FcH/FcH^+. [d]Decomposition temperature at 10% weight loss, determined by TGA.

Electrochemical propetries:

The electrochemical behaviour of the truxenes **6**, **7, 10** and **11** were investigated by the cyclic voltammetric analysis in dry dichloromethane solution at room temperature (25 °C) using tetrabutylammoniumhexafluorophosphate ($TBAPF_6$) as a supporting electrolyte. The electrochemical data are listed in Table **1**. The cyclic voltammograms of the truxenes **6**, **7, 10**

View Article Online
DOI: 10.1039/C7NJ03934D

and **11** are shown in the ESI section. All potentials are corrected to be referenced against FcH/FcH^+, as required by IUPAC.[27] The cylic voltammogram of the truxenes **6**, **10** and **11** show one irreversible oxidation wave in the range of 1.25–1.31 V (Figure **S1**). The triphenylamine substituted truxene **7** shows one reversible oxidation peak and one quasireversible peak. The first oxidation potentials of truxene **7** is at $E_{1/2}$ = 0.37 V, and the second oxidation potential at $E_{1/2}$ = 0.96 V, suggesting a successive formation of the monocation and then dication radical, which is attributed to the removal of electrons from the triphenylamine moiety.[28]

The truxenes **6**, **7, 10** and **11** exhibit one reversible reduction wave in the range of -1.44 to -1.49 V. The acceptor substituted truxenes **6**, **10**, and **11** exhibit harder oxidation and reduction as compared to donor substituted truxene **7**. This reflects strong donor-acceptor interaction in truxene **6**, **10** and **11**.

Time-Dependent Density Functional (TD-DFT) Studies:

To understand the photophysical and electrochemical properties of donor-acceptor substituted truxenes **6**, **7, 10** and **11** the density functional theory (DFT) and time dependent density functional (TD-DFT) calculations were performed. The structures **6**, **7, 10** and **11** were optimized using Gaussian 09 program at the B3LYP/6-31G** level.[29] The TD-DFT calculations were carried out in the 1,2-dichloroethane (DCE) using the polarized continuum model (CPCM) of Gaussian 09 software. The 6-31G**/CAM-B3LYP basis set was used for all the calculations.[29]

The TD-DFT predicted vertical excitation energies of truxene **6** and **7** are shown in Figure **6** (truxene **10** and **11** can be found in ESI Figure **S2**) along with experimental UV-vis spectra and data are listed in Table **2**. The truxene **6** shows absorption bands calculated at CAM-B3LYP level at 284 nm and 389 nm. The experimental values for these transitions are 320

View Article Online
DOI: 10.1039/C7NJ03934D

nm and 418 nm respectively. The truxene **7** shows calculated band at 272 nm and 355 nm which corresponds to experimental bands at 300 nm and 383 nm (Figure **6**). The incorporation of TCNE (truxene **10**) results major intense transitions at 383 nm and TCNQ (truxene **11**) results bands at 370 nm and 570 nm, which belongs to intramolecular charge transfer (ICT), this is in accordance with the experimental values (Figure **S2**). These bands are supported by the frontier molecular orbitals, which show that intramolecular charge transfer (ICT) takes place from triphenylamine (donor) to TCNE or TCNQ (acceptor) as shown in Figure **S4**.

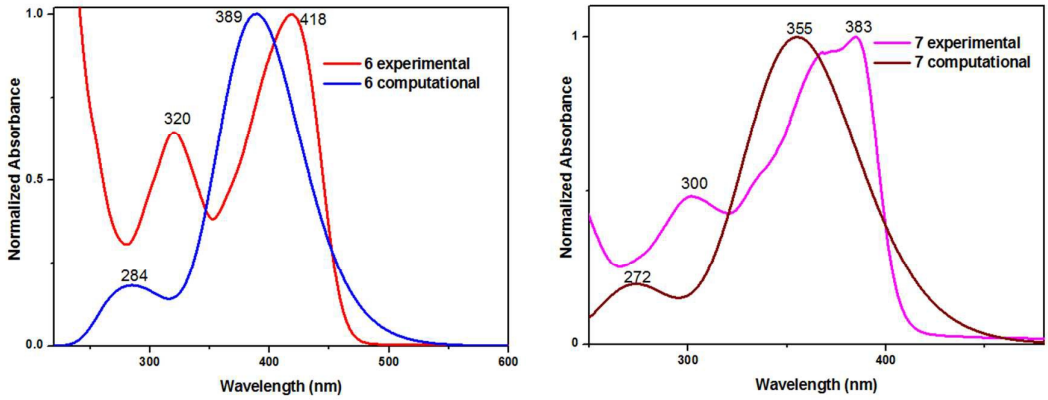

Figure 6. The comparison of experimental and calculated (TD-DFT at CAM-B3LYP level) absorption spectrum of truxene **6**, **7** in 1,2-dichloroethane solution.

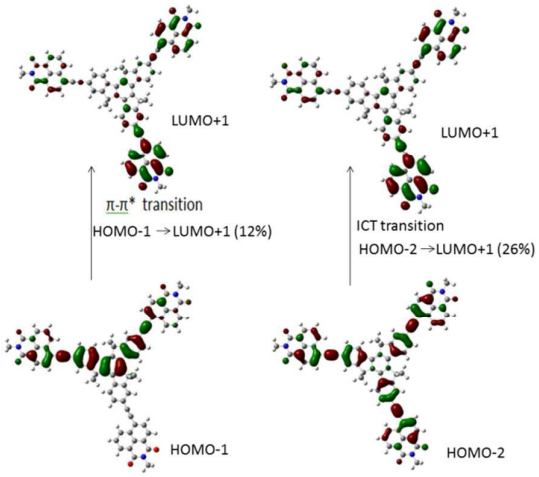

Figure 7. The major transitions in truxene **6**

View Article Online
DOI: 10.1039/C7NJ03934D

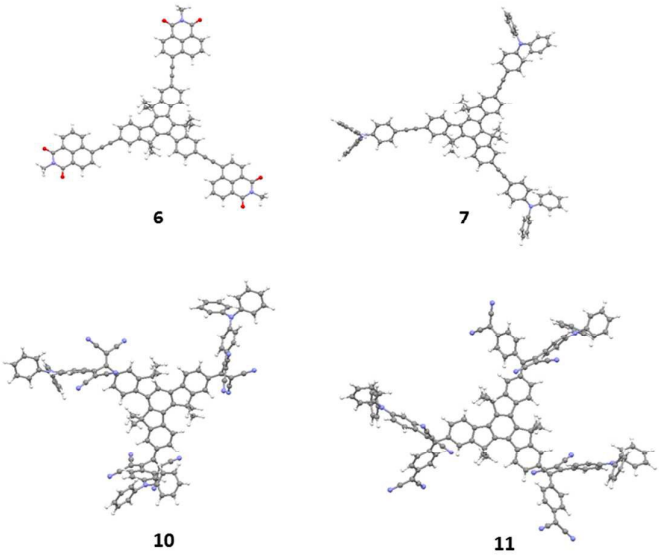

Figure 8. The DFT optimized structures of the truxenes **6**, **7, 10** and **11** with Gaussian 09 at the B3LYP/6-31G** level of theory.

Table 2. Computed vertical transition energies and their Oscillator strengths (*f*) and major contributions for the truxenes **6**, **7, 10** and **11**

Truxenes	TD-DFT/ CAM-B3LYP (DCE)		
	λ_{max}	f^{a}	**Major contribution** (%)
6	284 nm	0.0087	HOMO−1→LUMO+1(12%)
	389 nm	2.29	HOMO−2→LUMO+1(26%)
7	272 nm	0.352	HOMO−2→LUMO+9 (15%)
	355 nm	3.369	HOMO−2→LUMO (21%)
10	383 nm	0.6231	HOMO−4→LUMO+2 (12%)
11	370 nm	0.2677	HOMO−1→LUMO (27%)
	520 nm	0.7923	HOMO−5→LUMO (11%)

[a]f is Oscillator strengths

The optimized structures of truxene **6** and **7** exhibit planar conformation with respect to truxene core. The incorporation of the TCNE and TCNQ groups results in loss of planarity in truxene **10** and **11**. The dihedral angle between the triphenylamine groups and truxene core is 76.1°, 89.6°, 74.9° in truxene **10,** and 74.0°, 74.8°, 74.8° in truxene **11** (Figure **8**).

View Article Online
DOI: 10.1039/C7NJ03934D

Figure **9** shows the electron density distribution of the HOMO and LUMO of the truxenes **6**, **7, 10** and **11.** In truxene **6** the HOMO is delocalized on the truxene core and LUMO is on the naphthalimide unit, this separation of HOMO and LUMO results in strong charge transfer and low energy gap (2.98 eV). The truxene **7** shows that, the HOMO is delocalized over the triphenylamine groups, whereas the LUMO is delocalized on the tuxene core. In case of TCNE and TCNQ substituted truxene **10** and **11** the HOMO is delocalized over the triphenylamine group and LUMO is on TCNE and TCNQ acceptor unit respectively. Thus, the electron density transfers from triphenylamine groups (HOMO) to TCNE (LUMO) and TCNQ groups in truxene **10** and **11**. The HOMO-LUMO gap is lowest in truxene **11** as compared to other truxenes due to the incorporation of TCNQ as a strong acceptor.

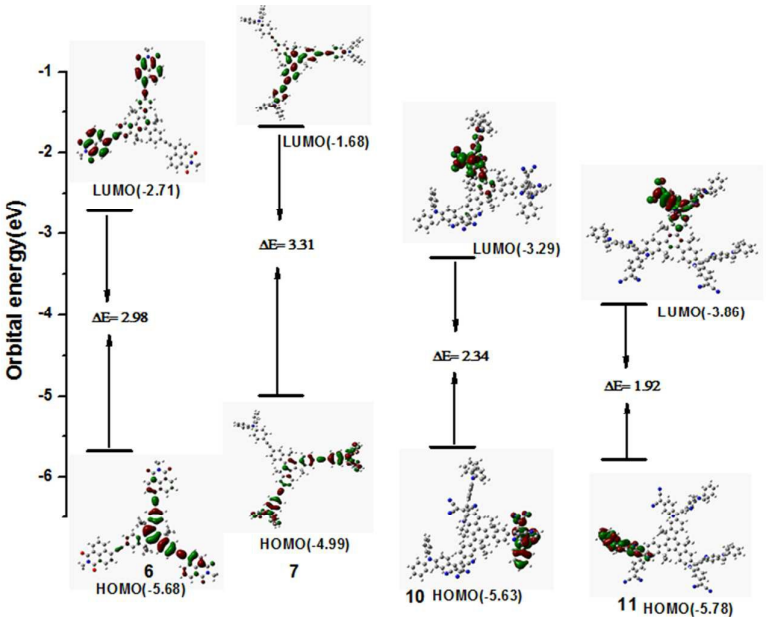

Figure 9. The energy level diagram of the frontier molecular orbitals of the truxenes **6**, **7, 10** and **11** calculated using B3LYP/6-31G(d,p) level of DFT theory.

View Article Online
DOI: 10.1039/C7NJ03934D

Conclusions

In summary, we have described the synthesis of star shaped donor-acceptor substituted truxenes **6**, **7, 10** and **11**. Their photophysical, electrochemical properties, thermal stability and HOMO-LUMO gap can be tuned by varying the strength of donor and acceptor groups. The optical properties of the truxenes **6**, **7, 10** and **11** were explained from the TD-DFT calculations. The computational calculation show significant lowering of the HOMO□ LUMO gap by the incorporation of TCNE and TCNQ groups in truxene **7**. The truxene **10** and **11** are non-emissive in nature which further supports strong donor–acceptor interaction. The thermal stability can be improved by the incorporation of planar naphthalimide unit on truxene core. The [2+2] cycloaddition retroelectrocyclization reaction pathway was studied by computational calculations. These studies show that, the donor substituted truxenes are favorable for the cycloaddition reaction whereas truxene substituted by acceptor groups are not favourable for [2+2] cycloaddition-retroelectrocyclization reactions. The results obtained here, provide a new avenue for the design and synthesis of organic molecules with low HOMO□LUMO gap and enhanced thermal stability for various optoelectronic applications. The study on photovoltaic properties of truxenes **6**, **7, 10** and **11** are currently in progress in our laboratory.

Experimental section

General experimental. All reagents were obtained from commercial sources, and used as received unless otherwise stated. ^{1}H NMR (400 MHz) and ^{13}C NMR (100 MHz) spectra were recorded on a Bruker Avance (III) 400 MHz instrument by using $CDCl_3$ as solvent. ^{1}H NMR chemical shifts are reported in parts per million (ppm) relative to the solvent residual peak ($CDCl_3$, 7.26 ppm). Multiplicities are given as s (singlet), d (doublet), t (triplet), q (quartet), and m (multiplet), and the coupling constants, *J*, are given in Hz. ^{13}C NMR chemical shifts are reported relative to the solvent residual peak ($CDCl_3$, 77.36 ppm). Thermogravimetric

View Article Online
DOI: 10.1039/C7NJ03934D

analyses were performed on the Mettler Toledo Thermal Analysis system. UV−visible absorption spectra were recorded on a Cary-100 Bio UV−visible spectrophotometer. Cyclic voltamograms (CVs) were recorded on a CHI620D electrochemical analyser using glassy carbon as the working electrode, Pt wire as the counter electrode, and the saturated calomel electrode (SCE) as the reference electrode. The scan rate was 100 mV s^{-1}. A solution of tetrabutylammonium hexafluorophosphate ($TBAPF_6$) in CH_2Cl_2 (0.1 M) was employed as the supporting electrolyte. DCM was freshly distilled from CaH_2 prior to use. All potentials were experimentally referenced against the saturated calomel electrode couple but were then manipulated to be referenced against FcH/FcH^+ as recommended by IUPAC. Under our conditions, the FcH/FcH^+ couple exhibited E° = 0.38 V versus SCE. HRMS was recorded on Bruker-Daltonics micrOTOF-Q II mass spectrometer.

Synthesis and Characterization

The reactants **4** and **5** were synthesized according to known methods.[21]

Procedure for the preparation of truxenes 6 and 7.

A solution of tri-iodotruxene **3** (250 mg, 0.20 mmol) and the corresponding alkyne (4.5 equivalent) in toluene–triethylamine 5 : 1 (60 mL) was deareated for 30 min with argon bubbling and then $Pd(dba)_2$ (40 mg, 0.07 mmol) and $AsPh_3$ (170 mg, 0.55 mmol) were added. The solution was deareated for a further 5 min. The mixture was heated at 80 ºC for 48 h. The solvent was removed; the remaining residue was suspended in water (50 mL) and extracted with DCM (3 x 20 mL). The combined organic layers were dried ($MgSO_4$) and concentrated in vacuum. The resulting crude product was purified by column chromatography on silica gel eluting with CH_2Cl_2/hexane (10%). The desired compounds obtained from the column was

View Article Online
DOI: 10.1039/C7NJ03934D

recrystallized from DCM/methanol to give compound **6** and **7** in 70% and 75% yield respectively.

Procedure for the preparation of truxenes 10 and 11.

A solution of alkyne derivative (40 mg) and TCNE/TCNQ (5 equivalent) in 1,2-dichloroethane was refluxed for 24 h at 100 ^{o}C. After completion of the reaction, the reaction mixture was concentrated under reduced pressure. The crude compound was purified by column chromatography on silica eluting with CH_2Cl_2/hexane (10%) and crystallized multiple times with DCM/methanol to afford truxene **10** and **11** in 71% and 65% yield.

Truxene 6: yellow solid (yield: 70%), M. P. above 280 °C. IR data (KBr, cm^{-1})- 754, 815, 854, 1083, 1381, 1661, 1701, 2159. ^{1}H NMR (400 MHz, $CDCl_3$): δ (ppm) 8.86 (d, 3H, *J* = 8.18 Hz,-naphthalimide core protons), 8.69 (d, 3H, *J* = 7.36 Hz,-naphthalimide core protons), 8.61 (d, 3H, *J* = 7.77 Hz,-naphthalimide core protons), 8.46 (d, 3H, *J* = 8.45 Hz, -naphthalimide core protons), 8.05 (d, 3H, *J* = 7.77 Hz-truxene core protons), 7.90 (t, 3H,-naphthalimide core protons), 7.76-7.82 (m, 6H, truxene core protons), 4.21 (t, 6H, N-butul chain protons), 2.94-3.01 (m, 6H, truxene hexyl chain protons), 2.14-2.25 (m, 6H, truxene hexyl chain protons), 1.70-1.80 (m, 6H, N-butyl chain protons), 1.41-1.51 (m, 6H, N-butul chain protons), 0.80-1.05 (m, 45H, truxene hexyl chain and methyl protons of butyl chain), 0.47-0.68 (m, 30H, truxene hexyl chain protons) ^{13}C NMR (100 MHz, $CDCl_3$): δ = 164.0, 163.8, 153.9, 146.6, 141.1, 138.0, 132.4, 131.6, 130.8, 130.5, 130.4, 128.2, 127.7, 127.4, 125.5, 124.7, 123.1, 122.1, 120.3, 99.9, 87.0, 56.07, 40.0, 37.0, 31.5, 30.2, 29.7, 29.4, 24.0, 22.2, 20.4, 13.9, 13.8. HRMS (ESI) m/z, calcd for M^+ ($C_{117}H_{129}N_3O_6$): 1671.9981; found: 1671.9994.

Truxene 7: brown solid (yield: 75%), M.P. 130 °C, IR data (KBr, cm^{-1})- 617, 648, 695, 2160. ^{1}H NMR (400 MHz, $CDCl_3$): δ (ppm) 8.31 (d, 3H, *J* = 8.91 Hz, truxene core protons), 7.52-7.61 (m, 6H, truxene core protons), 7.44 (d, 6H, *J* = 7.80 Hz, triphenyl amine core

View Article Online
DOI: 10.1039/C7NJ03934D

protons), 7.24-7.32 (m, 12H, triphenyl amine core protons), 7.01-7.06 (m, 24H, triphenyl amine core protons), 2.85-2.91 (m, 6H, hexyl chain protons), 2.00-2.15 (m, 6H, hexyl chain protons), 0.77-0.91 (m, 36H, hexyl chain protons), 0.39-0.66 (m, 30H, hexyl chain protons). ^{13}C NMR (100 MHz, $CDCl_3$): δ = 153.6, 147.9, 147.2, 145.7, 140.0, 138.0, 132.5, 129.4, 129.7, 125.0, 124.4, 123.5, 122.3, 121.2, 116.2, 99.0, 89.4, 55.7, 36.9, 31.5, 29.6, 29.4, 23.9, 22.2, 13.8. HRMS (ESI) m/z, calcd for M^+ ($C_{123}H_{129}N_3$): 1649.0214; found: 1649.0620.

Truxene 10: Reddish brown solid (yield: 71%), M. P. above 280 °C. IR data (KBr, cm^{-1})- 803, 748, 1185, 1337, 1466, 1443, 2158, 2221. ^{1}H NMR (400 MHz, $CDCl_3$): δ (ppm) 8.44 (d, 3H, *J* = 8.01 Hz, TPA core protons), 8.17 (s, 3H, truxene core protons), 7.77 (d, 6H, *J* = 9.01 Hz, truxene core protons),7.37-7.50 (m, 13H, Triphenyl amine core protons), 7.20-7.32 (m, 20H, Triphenyl amine core protons), 6.99 (d, 6H, *J* = 10.01 Hz, Triphenyl amine core protons), 2.79-2.91 (m, 6H, hexyl chain protons), 2.11-2.24 (m, 6H, hexyl chain protons), 0.74-0.98 (m, 36H, hexyl chain protons), 0.35-0.60 (m, 30H, hexyl chain protons). ^{13}C NMR (100 MHz, $CDCl_3$): δ = 168.6, 163.8, 154.6, 153.9, 150.0, 145.3, 144.4, 137.5, 132.0, 130.5, 130.1, 128.3, 126.9, 126.8, 125.5, 124.0, 121.7, 118.0, 113.6, 112.6, 112.4, 111.4, 86.3, 78.0, 56.8, 36.7, 31.4, 29.1, 24.0, 22.1, 13.8. HRMS (ESI) m/z, calcd for M^+ ($C_{141}H_{129}N_{15}$): 2032.0555; found: 2032.1007.

Truxene 11: Black solid (yield: 65%), M. P. above 280 °C. IR data (KBr, cm^{-1})- 695, 755, 815, 1177, 1575, 2209. ^{1}H NMR (400 MHz, $CDCl_3$): δ (ppm) 8.37 (d, 3H, *J* = 9.23 Hz, TPA core protons), 7.90 (s, 3H, truxene core protons), 7.65 (d, 3H, *J* = 9.80 Hz, truxene core protons), 7.58 (d, 3H, *J* = 9.80 Hz, triphenyl amine core protons), 7.29-7.38 (m, 15H, triphenyl amine core protons), 7.19-7.25 (m, 12H, triphenyl amine core protons), 7.13-7.19 (m, 15H, triphenyl amine core protons), 7.04 (d, 3H, *J* = 10.38 Hz, triphenyl amine core protons), 6.97 (d, 6H, *J* = 9.23 Hz, triphenyl amine core protons), 2.74-2.86 (m, 6H, hexyl chain protons), 1.99-2.10 (m, 6H, hexyl chain protons), 0.72-0.91 (m, 36H, hexyl chain

View Article Online
DOI: 10.1039/C7NJ03934D

protons), 0.32-0.56 (m, 30H, hexyl chain protons).

^{13}C NMR (100 MHz, $CDCl_3$): δ = 171.4, 154.5, 153.7, 151.6, 150.5, 149.5, 145.2, 140.6, 137.5, 135.2, 134.0, 133.4, 133.0, 132.7, 129.9, 128.5, 127.1, 126.5, 126.0, 125.4, 123.7, 119.1, 114.0, 113.8, 113.3, 112.3, 86.6, 74.8, 56.5, 53.4, 36.5, 31.2, 28.9, 23.9, 22.0, 13.8. HRMS (ESI) m/z, calcd for M^+ ($C_{159}H_{141}N_{15}$): 2261.1521; found: 2261.2406.

Supporting Information

The ^{1}H NMR, ^{13}C NMR spectra, mass spectroscopy data, cyclic voltammograms, UV-vis graphs, and DFT calculations of truxenes **6**, **7, 10** and **11** are provided.

Corresponding Author

*E-mail: rajneeshmisra@iiti.ac.in.

Tel.: +91 7312438754; fax: +91 7312361482.

Acknowledgements

We acknowledge support by INSA (Project No. SP/YSP/139/2017/2293), Department of Science and Technology (Project No. EMR/2014/001257), and Council of Scientific and Industrial Research (Project No. 01/(2795)/14/EMR-II), New Delhi for the financial support. We also thank the Sophisticated Instrumentation Centre (SIC), Indian Institute of Technology (IIT) Indore.

References:

1. (a) P. Sonar, S. P. Singh, Y. Li, M. S. Soh and A. Dodabalapur, *Adv. Mater.* 2010, **22**, 5409−5413. (b) S. Kato, T. Furuya, A. Kobayashi, M. Nitani, Y. Ie, Y. Aso, T. Yoshihara, S. Tobita and Y. Nakamura, *J. Org. Chem.* 2012, **77**, 7595−7606. (c) K. M. Omer, S. Y. Ku, K. T. Wong and A. J. Bard, *J. Am. Chem. Soc.*, 2009, **131**, 10733−10741. (d) Y. Li, A. Li, B.-X. Huang, J. Zhao, B.-Z. Wang, J.-W. Li, X.-H. Zhu, J. Peng, Y. Cao and D. G. M. Roncali, *J.*

View Article Online
DOI: 10.1039/C7NJ03934D

Org. Lett., 2009, **11**, 5318−5321. (e) J. L. Wang, Z.-M. Tang, Q. Xiao, Y. Ma and J. Pei, *Org. Lett*. 2009, **11**, 863−866. (f) R. Sharma , R. Margani , S. M. Mobin and R. Misra, *RSC Adv*., 2013, **3**, 5785–5788. (g) C. P. Singh, R. Sharma, V. Shukla, P. Khundrakpam, R. Misra, K.S. Bindra, R. Chari, *Chem. Phys. Lett.*, 2014, **616**, 189–195.

2 (a) S. Kato, T. Matsumoto, T. Ishi-i, T. Thiemann, M. Shigeiwa, H. Gorohmaru, S. Maeda, Y. Yamashitad and S. Mataka, *Chem. Commun*., 2004, 2342−2343. (b) B. A. D. Neto, A. A. M. Lapis, E. N. da S. Júnior and J. Dupont, *Eur. J. Org. Chem*. 2013, 228−255. (c) S. Kato, T. Matsumoto, M. Shigeiwa, H. Gorohmaru, S. Maeda, T. Ishi-I and S. Mataka, *Chem. Eur. J.,* 2006, **12**, 2303−2317. (d) N. Kobayashi, S. Inagaki, V. N. Nemykin and T. Nonomura, *Angew. Chem., Int. Ed.,* 2001, **40**, 2710−2712. (e) B. D. Lindner, J. U. Engelhart, M. Märken, O. Tverskoy, A. L. Appleton, F. Rominger, K. I. Hardcastle, M. Enders and U. H. F. Bunz, *Chem. Eur. J.,* 2012, **18**, 4627−4633. (f) A. Aviram and M. A. Ratner, *Chem. Phys. Lett.* 1974, **29**, 277−283. (g) R. Sharma, P. Gautam, S. M. Mobin and R. Misra, *Dalton Trans.,* 2013, **42**, 5539–5545. (h) R. Sharma, P. Gautam, R. Misra and S. K. Shukla, *RSC Adv*., 2015, **5**, 27069.

3. (a) Q. T. Zhang and J. M. Tour, *J. Am. Chem. Soc.*, 1998, **120**, 5355−5362. (b) F. Gohier and P. R. Frère, *J. Org. Chem.*, 2013, **78**, 1497–1503. (c) R. Sharma, R. Maragani and R. Misra, *J. Organomet. Chem.,* 2016, **825**, 8–14.

4. (a) M. Štefko, M. D. Tzirakis, B. M. O. Ebert, O. Dumele, W. B. Schweizer, J. P. Gisselbrecht, C. Boudon, M. T. Beels, I. Biaggio and F. Diederich, *Chem. –Eur. J.*, 2013, **19**, 12693–12704. (b) H. A. M. van, J. A. Mullekom, J. M. Vekemans and E. W. Meijer, *Chem. −Eur. J.*, 1998, **4**, 1235–1243. (c) J. L. Wang and Q. Xiao, J. Pei, *Org.Lett*., 2010, **12**, 4164–4167. (d) F. Bures, W. B. Schweizer, J. C. May, C. Boudon, J. P. Gisselbrecht, M. Gross, I. Biaggio and F. Diederich, *Chem.−Eur. J.*, 2007, **13**, 5378–5387. (e) N. N. P. Moonen, W. C.

View Article Online
DOI: 10.1039/C7NJ03934D

Pomerantz, R. Gist, C. Boudon, J. P. Gisselbrecht, T. Kawai, A. Kishioka, M. Gross, M. Irie and F. Diederich, *Chem. −Eur. J.*, 2005, **11**, 3325–3341.

5. P.; Gautam, R. Misra, S. A. Siddiqui and G. D. Sharma, *ACS Appl. Mater. Interfaces*, 2015, **7**, 10283–10292.

6. (a) M. Kivala and F. Diederich, *Acc. Chem. Res*., 2009, **42**, 235–248; (b) S. Kato and F. Diederich, *Chem. Commun*., 2010, **46**, 1994–2006. (c) M. Kivala, T. Stanoeva, T. Michinobu, B.; Frank, G. Gescheidt and F. Diederich, *Chem.–Eur. J*., 2008, **14**, 7638–7647.

7. (a) T. Michinobu, J. C. May, J. H. Lim, C. Boudon, J. P. Gisselbrecht, P. Seiler, M. Gross, I. Biaggio and F. Diederich, *Chem. Commun*., 2005, 737–739. (b) T. Michinobu, I. Boudon, J. P. Gisselbrecht, P. Seiler, B. Frank, N. N. P. Moonen, M. Gross and F. Diederich, *Chem.–Eur. J.,* 2006, **12**, 1889–1905. (c) A. Leliège, P. Blanchard, T. Rousseau and J. Roncali, *Org. Lett.,* 2011, **13**, 3098–3101.

8. (a) T. Michinobu, N. Satoh, J. Cai, Y.; Lia and L. Hanb, *J. Mater. Chem. C*, 2014, **2**, 3367–3372. (b) B. Esembeson, M. L. Scimeca, T. Michinobu, F. Diederich and I. Biaggio, *Adv. Mater.*, 2008, **20**, 4584–4587.

9. (a) M. Yamada, W. B. Schweizer, F. Schoenebeck and F. Diederich, *Chem. Commun.* 2010, **46**, 5334–5336. (b) M. Jordan, M. Kivala, C. Boudon, J.□P. Gisselbrecht, W. B. Schweizer, P. Seiler and F. Diederich, *Chem.–Asian J.,* 2011, **6**, 396–401. (c) M. Kivala, C. Boudon, C. Gisselbrecht, P. Seiler, M. Gross and F. Diederich, *Chem. Commun*., 2007, 4731–4733. (d) T. Michinobu, *J. Am. Chem. Soc.* 2008, **130**, 14074–14075. (e) Y. Li and T. Michinobu, *Macromolecules*, 2010, **43**, 5277–5286. (f) T. Shoji, S. Ito, K. Toyota, M. Yasunami and N. Morita, *Chem.–Eur. J.,* 2008, **14**, 8398–8408. (g) T. Shoji, S. Ito, K. Toyota, T. Iwamoto, M. Yasunami and N. Morita, Eur. *J. Org. Chem*., 2009, 4316–4324. (h) N. Krauße, M. Kielmann, J. Ma and H. Butenschön, *Eur. J. Org. Chem.* 2015, 2622–2631.

View Article Online
DOI: 10.1039/C7NJ03934D

10. (a) T. Jadhav, R. Maragani, R. Misra, V. Sreeramulu, D. N. Rao and S. M. Mobin, *Dalton Trans.*, 2013, 42, 4340–4342. (b) P. Gautam, B. Dhokale, S. M. Mobin and R. Misra, *RSC Adv.*, 2012, **2**, 12105–12107. (c) R. Misra, R. Sharma and S. M. Mobin, *Dalton Trans.*, 2014, **43**, 6891–6896.

11. (a) B. Ventura, A. Barbieri, F. Barigelletti, S. E. Diring and R. Ziessel, *Inorg. Chem.* 2010, **49**, 8333–8346. (b) F. Goubard and F. Dumur, *RSC Adv.*, 2015, **5**, 3521-3551.

12. (a) W. B. Zhang, W. H. Jin, X. H. Zhoua and J. Pei, *Tetrahedron*, 2007, **63**, 2907–2914. (b) J. Huang, B. Xu, J. H. Su, H. Chin and H. Tian, *Tetrahedron*, 2010, **66**, 7577–7582.

13. (a) M. M. Boorum, Y. V. Vasil, T. Drewello and L. T. Scott, *Science*, 2001, **294**, 828. (b) B. Gomez-Lor, O. De Frutos and A. M. Echavarren, *Chem. Commun.*, 1999, 2431. (c) P. W. Rabideau, A. H. Abdourazak, Z. Marcinow, R. Sygula and A. Sygula, *J. Am. Chem. Soc.* 1995, **117**, 6410. (d) E. V. Demlow and T. Kelle, *Synth. Commun.* 1997, **27**, 2021. (e) B. Gomez-Lor, E. Gonzalez-Cantalapiedra, O. DeFrutos, C. Ardenas, D. J. Santos and A. M. Echavarren, *Chem. Eur. J.*, 2004, **10**, 2601.

14. J. Pei, J. L. Wang, X. Y. Cao, X. H. Zhou and W. B. Zhang, *J. Am. Chem. Soc.*, 2003, **125**, 9944. (b) X. Y. Cao, W. B. Zhang, J. L. Wang, X. H. Zhou, H. Lu and J. Pei, *J. Am. Chem. Soc.*, 2003, **125**, 12430.

15. (a) X. Zong, M. Liang, C. Fan, K. Tang, G. Li, Z. Sun and S. Xue, *J. Phys. Chem. C.,* 2012, **116**, 11241−11250. (b) Y. Xie, X. Zhang, Y. Xiao, Y. Zhang, F. Zhou, J. Qib and J. Qu, *Chem. Commun.*, 2012, **48**, 4338–4340. (C) Z. Yang, B. Xu, J. He, L. Xue, Q. Guo, H. Xia and W. Tian, *Org. Elec.*, 2009, **10**, 954–959.

16. (a) H. J. Xua, B. Dub, C. P. Gros, P. Richarda, J. M. Barbea. and D. H. Pierre, *J. Porphyrins Phthalocyanines,* 2013, **17**, 44–55. (b) M. Kimura, S. Kuwano, Y. Sawaki, H. Fujikawa, K. Noda, Y. Taga and K. Takagi, *J. Mater. Chem.*, 2005, **15**, 2393–2398. (C) M. S. Yuan, Z. Q. Liu and Q. Fang, *J. Org. Chem.*, 2007, **72**, 7915–7922.

View Article Online
DOI: 10.1039/C7NJ03934D

17. (a) W. Huang, E. Smarsly, J. Han, M. Bender, K. Seehafer, I. Wacker, R. R. Schröder and U. H. F. Bunz, *ACS Appl. Mater. Interfaces*, 2017, **9**, 3068–3074. (b) R. Misra and P. Gautam, *Org. Biomol. Chem.*, 2014, **12**, 5448–5457. (c) L. Ma, W. Zhaoxin, Z. Guijiang, Y. Fang, Y. Yue, Y. Chunliang, N. Shuya, H. Xun, L. Yu, W. Shufeng and G. Qihuang, *J. Mater. Chem. C*, 2015, **3**, 7004–7013.

18. D. Lehnherr, M. Adam, A. H. Murray, R. McDonald, F. Hampel and R. R. Tykwinski, *Canadian Journal of Chemistry*, 2017, **95**, 303–314.

19. A. L. Kanibolotsky, R. Berridge, P. J. Skabara, I. F. Perepichka, D. D. C. Bradley and M. Koeberg, *J. Am. Chem. Soc.,* 2004, **126**, 13695.

20. X. Cao, H. Zi, W. Zhang, H. Lu and J. Pei, *J. Org. Chem*., 2005, **70**, 3645-3653.

21. R. Maragani, S. Bijesh, R. Sharma and R. Misra, *Asian J. Org. Chem.* 10.1002/ajoc.201700274.

22. V. Benin, A. T. Yeates and D. Dudis, *J. Heterocyclic Chem.,* 2008*,* **45**, 811.

23. P. Reutenauer, M. K. Peter, D. Jarowski, C. Boudon, J. P. Gisselbrecht, M. Grossb and F. Diederich, *Chem. Commun*., 2007, 4898–4900.

24. S. Chen, Y. Li, C. Liu, W. Yang and Y. Li, *Eur. J. Org. Chem*., 2011, **32**, 6445–6451.

25. (a) B. Dhokale, P. Gautam and R. Misra, *Tetrahedron Lett.,* 2012, **53**, 2352–2354. (b) J. Rochford and M. T. P. Rooney, *Inorg. Chem*., 2007, **46***,* 7247. (c) M. R. Rao, K. V. Pavan and M. Ravikanth, *J. Organomet. Chem*., 2010, **695**, 863–869.

26. (a) S. Fery-Forgues and J. Delavaux-Nicot, *J. Photochem. Photobiol., A*, 2000, **132**, 137–159. (b) V. A. Nadtochenko, N. N. Denisov, V. Y. Gak, N. V. Abramova and N. M. Loim, *Russ. Chem. Bull.*, 1999, **148**, 1900. (c) S. Barlow and S. R. Marder, *Chem. Commun.*, 2000, 1555–1562.

View Article Online
DOI: 10.1039/C7NJ03934D

27. (a) F. Francl, W. J. Pietro, W. J. Hehre, J. S. Binkley, M. S. Gordon, D. J. Defrees and J. A. Pople, *J. Chem. Phys.*, 1982, **77**, 3654–3665. (b) F. Ding, S. Chen and H. Wang, *Materials,* 2010*,* **3**, 2668–2683.

28. Z. Yang, B. Xu, J. He, L. Xue, Q. Guo, H. Xia and W. Tian, *Organic Electronics,* 2009, **10**, 954–959.

29. A. Pedone, *J. Chem. Theory Comput*., 2013, **9**, 4087−4096.